Nuclear Inst. and Methods in Physics Research, A 1034 (2022) 166767

Contents lists available at ScienceDirect

Nuclear Inst. and Methods in Physics Research, A

journal homepage: www.elsevier.com/locate/nima

Thick target neutron spectral yield and dose measurements with ^{nat}C (p, n) system at intermediate proton energies between 8–20 MeV

Sabyasachi Paul [a,*], Meghnath Sen [b,c], S.S. Ghodke [b], A.A. Shanbhag [a], S.P. Tripathy [a,c], G.S. Sahoo [a], S.C. Sharma [d], N.G. Ninawe [d], Y. Singh [b], R.B. Rakesh [b], M.S. Kulkarni [a,c]

[a] Health Physics Division, Bhabha Atomic Research Centre, Mumbai, India
[b] Radiation Safety Systems Division, Bhabha Atomic Research Centre, Mumbai, India
[c] Homi Bhabha National Institute, Anushaktinagar, Mumbai, India
[d] Nuclear Physics Division, Bhabha Atomic Research Centre, Mumbai, India

ARTICLE INFO

Keywords:
Neutron spectrometry
Thick target neutron yield
Graphite target
Neutron dosimetry
^{13}C (p, n) reaction

ABSTRACT

The study of neutron parameters from a thick natural graphite target is of immense importance for obtaining the background neutron energy and yield corrections in case of proton irradiation of low Z targets, where graphite is used predominantly as the supporting target material. There are few measurements with thick graphite target reported in literature at proton energies up to 12 MeV and some at higher energies beyond 20 MeV. The present study focuses on the thick target neutron yield, dose and spectra measurements from thick ^{nat}C(p,n) system at intermediate proton energies between 8–20 MeV. The experimental measurements were performed at 0° and 90° with respect to the incident beam direction. The generated data will complement the discontinuity in the neutron yield and spectral measurements, in the proton energy range of 12–20 MeV. These dosimetric estimates in the proton energy range of 8–20 MeV will be significant towards the personal radiation protection of occupational workers and neutron shielding evaluations.

1. Introduction

In recent years, the accelerated proton induced nuclear reactions with low mass targets are extensively used for production of high energy quasi mono-energetic neutrons (QMN) for various applications viz., materials characterization [1], materials damage studies [2], calibration of the radiation detectors for existing and upcoming high energy accelerators fields [3]. The proton induced reactions on the low Z targets like Li, Be, B or C isotopes are extensively studied for cross-section measurements [4,5] and other nuclear physics studies. These experiments were conducted at both energy regimes, i.e., near the Coulomb barrier and at high energies with targets either as pure metals or in the form of chemical salt with isotopic enrichment. In most of the cases, the targets are not self-supporting and needs backing material during the process of irradiations. At intermediate proton energies of 5–20 MeV, the high Z thick targets like tantalum [6–8], tungsten or gold are not good choices as supporting materials considering the high neutron yields beyond proton energies of 6 MeV [9]. In these experiments, thick natural graphite targets can be an optimum choice as backing material. In case of carbon isotopes, the dominant ^{12}C isotope (98.93%) has high neutron emission threshold (>19.5 MeV) resulting in low neutron yields compared to high Z targets. With graphite target the emission neutron contributions from the ^{13}C (natural abundance: 1.07%) isotope exists with a threshold of 3.23 MeV but the total neutron yield will be less based on abundance fraction. Considering this advantage of graphite, it is already in use as backing target for Li(p,n) reaction based QMN generation facilities at Universite Catholique de Louvain (UCL), Belgium [10]; CYRIC, Japan [11] and at NPI, Rez, CZ [12]. Apart from the QMN facilities, the positron emission tomography (PET)-cyclotron facilities also extensively uses the carbon based Faraday cups as the beam stopper [13]. Considering these uses of natural carbon targets at QMN, PET cyclotron facilities and in experiments using low Z targets at different proton energies, the study of thick target neutron yield and the dosimetric quantification in the intermediate energies becomes extremely important. Based on the available literatures, the thick target neutron yield (TTNY) measurements for natural carbon targets under proton irradiations are sparsely available [14] till the proton energies up to 12 MeV. Similarly, some cross-section measurements [5,15] and theoretical estimates [16] are available up to this energy range considering negligible contribution from the dominant ^{12}C isotope. Some proton and deuteron induced reactions with the carbon targets were reported at higher energies [17,18] with one TTNY measurement at 20 MeV protons [19]. These reports indicate a data void in the TTNY measurements between 12–20 MeV

* Correspondence to: 1-213-H, Modular Laboratory, Health Physics Division, Bhabha Atomic Research centre, Mumbai 400085, Maharashtra, India.
E-mail address: spaul@barc.gov.in (S. Paul).

https://doi.org/10.1016/j.nima.2022.166767
Received 4 February 2022; Received in revised form 13 April 2022; Accepted 18 April 2022
Available online 26 April 2022
0168-9002/

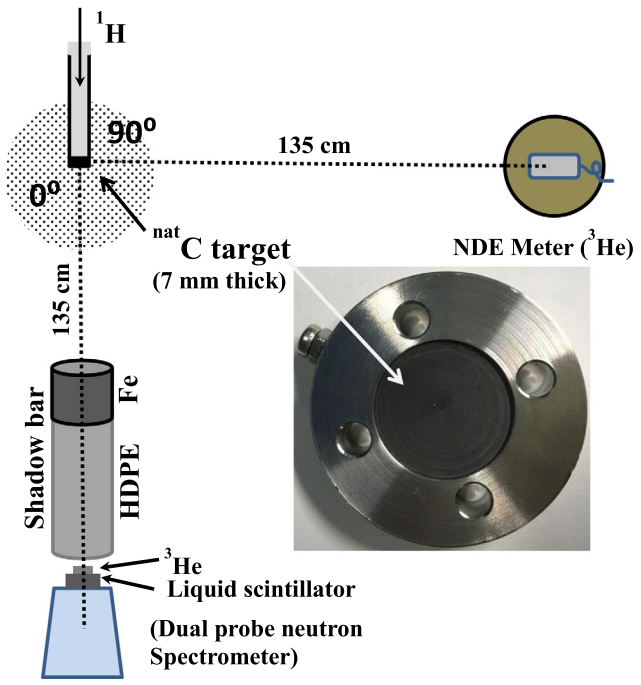

Fig. 1. The experimental set up with relative position of the detectors and the target assembly.

protons on a thick natural carbon target. Considering this need, in the present work, a systematic measurement of the thick target neutron spectra, yield and angular variations at 0° and 90° with respect to the incident beam direction has been carried out in the intermediate proton energy range between 8–20 MeV. The energy overlap of 8–12 MeV has been kept in the present work for comparison of the thick target neutron yields with the available literature data. The neutron spectra measured with the present method has also been compared with the available emission neutron data reported in the earlier measurements [14,19]. The comparison of the neutron ambient dose equivalent ($H^*(10)$) estimates using the neutron dose equivalent (NDE) meter and from the recorded spectra has also been presented at both the angles. The present study provides the neutron yield and dose measurements in the proton energy interval between 12–20 MeV for the ^{nat}C (p, n) system.

2. Materials and methods

In the present experiment, the proton beam was taken at the 30° N beam line in the Pelletron experimental hall of the BARC-TIFR Pelletron-LINAC facility. The proton energy was varied between 8 to 20 MeV with an energy interval of 2 MeV and the current was kept ~8–10 nA during the entire experiment. A Thick carbon block of 7 mm thickness with natural isotopic abundance (^{12}C: 98.93% and ^{13}C:1.07%) embedded in a stainless steel flange is used as the target assembly. The SRIM [20] estimated range of 20 MeV ^{1}H beam on the solid carbon target is 2.1 mm. So, a 7 mm thick graphite block can be considered as a stopping target with more than 3 times thickness compared to the particle range in the medium. At lower energies, it will automatically serve as an infinite thickness ^{nat}C block.

The emission neutron spectra from the ^{nat}C (p, n) system were measured using a dual detector based compact neutron probe (N-probe, BTI, Canada). The spectrometer uses a ^{3}He detector for thermal neutron detection and a $2'' \times 2''$ liquid scintillator (NE-213) with pulse height unfolding for fast neutrons, in the energy range between 800 keV to 20 MeV. The neutron spectrum generation from the raw outputs of the detectors were carried out using the Microspec-6 (ver. 6.5.6) analyzer module. The ^{3}He probe has been calibrated using a moderated ^{252}Cf source and the channel calibration of the fast neutron probe was carried out using a standard ^{24}Na (511 keV and 1274.5 keV) source. Before the proton beam experiments, multiple background dataset were generated in the "beam off" condition. The background spectra indicated 1%–2% contribution in the low energies below 0.5 MeV compared to the responses at the "beam on" condition; and at higher energies, the background was found to be almost zero. The net neutron spectra at specified proton energies were obtained after the background corrections. The ambient dose equivalent measurements were carried out using the NDE meter (Berthold LB 6411, Germany) calibrated to the $H^*(10)$ for neutrons. Both spectrometric and dosimetric measurements were carried out at 135 cm distance from the source, and in both 0° and 90° directions with respect to the incident beam. The detail of the experimental setup is shown in Fig. 1. During the spectrometric measurements, the scattered neutron contribution was measured in both angles at each energy by placing a shadow bar (19 cm Fe followed by a 42 cm high density polyethylene cylinders) in front of the detector assembly. This scattered fraction has been subtracted from the direct measurements to obtain the net neutron response at a specified energy and angle, per unit incident charge of protons deposited on the target. The cumulative charge deposited during the experiment was measured using a charge integrator. However, for the radiation protection aspects, the neutron ambient dose equivalent measurements using the NDE meter were carried out without any shadow shield considering the real field radiation environment.

3. Results and discussion

The neutron generation from the thick natural carbon target upon interaction with protons depends on the threshold of neutron emitting reactions from available isotopes. Natural carbon contains primarily two isotopes, ^{12}C (98.93%) and ^{13}C (1.07%) with traces of ^{14}C (~ 1 part per trillion). Among these, major isotope ^{12}C is expected to have small contribution in the total neutron yield till proton energy of 20 MeV due to its high reaction thresholds of 19.64, 20.29 MeV for (p,n) and (p, np) reactions respectively. The ^{14}C (p, n) reactions are feasible in the proton energy range under study. So, the expected major contributor for the emitting neutron fluence in the present system is ^{13}C. This isotope contains direct neutron emitting reaction and multiple breakup pathways for neutron emission at lower threshold energies. The corresponding thresholds for different reactions are listed in Table 1. The Table clearly indicates that, ^{13}C(p, n) and (p, np) reactions have the lowest threshold among the contributing reactions and will play a significant role at each proton energy under study. The breakup reactions have a higher threshold and the neutron contributions from these multiple α-emission reactions will contribute only at energies more than 14 MeV. Considering multiple neutron emission channels available for the system under study, identification of the major contributors based on the emission cross-sections become crucial.

The ^{13}C(p, n) reaction cross-sections in the proton energy range of 8–20 MeV is shown in Fig. 2 as black squares. The maximum measured cross-sections [21] for this reaction is ~200 mb around 6.5 MeV and reaches a steady value ~30-40 mb at proton energies beyond 12 MeV. The dotted line in the plot indicates the average cross-section variation with proton energy and is solely for visual representation. Being a thick target measurement, the energy degradation taking place in the interior volume of the target will emit more number of neutrons considering the higher emission cross-sections at lower energies. Consequently though cross-section reduces with increasing proton energy, still the total neutron yield will increase with increasing incident proton energies in the thick carbon, considering the proton energy degradation in the stopping target. Apart from ^{13}C(p, n) reaction, the measured or evaluated cross-sections for other neutron emission pathways were found insignificant in the proton energy range of 8–20 MeV and the contributions can be neglected. The threshold for ^{14}C(p, n) reaction is

Table 1
Tentative neutron emitting reaction thresholds from the natural carbon target with 20 MeV protons.

Isotope	Abundance	Reaction	Threshold (MeV)
^{12}C	98.93%	^{12}C+^{1}H → ^{12}N+n	19.64
		→ ^{11}C+n+p	20.29
^{13}C	1.07%	^{13}C+^{1}H → ^{13}N+n	3.24
		→ ^{12}C+n+p	5.33
		→ ^{4}He+n+p+2α	13.16
		→ ^{8}Be+n+p+α	13.26
		→ ^{9}Be+n+α	13.46
		→ ^{5}Li+n+2α	15.29
^{14}C	Trace (~1 ppt)	^{14}C+^{1}H → ^{14}N+n	0.67

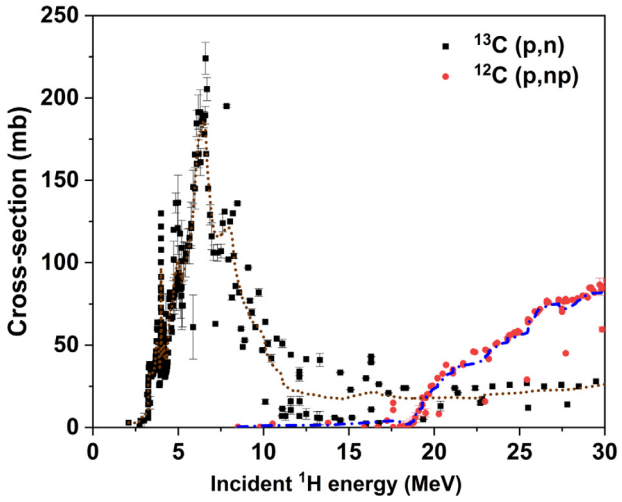

Fig. 2. Measured cross-sections of ^{13}C(p, n) and ^{12}C(p, np) reactions from EXFOR [21] database.

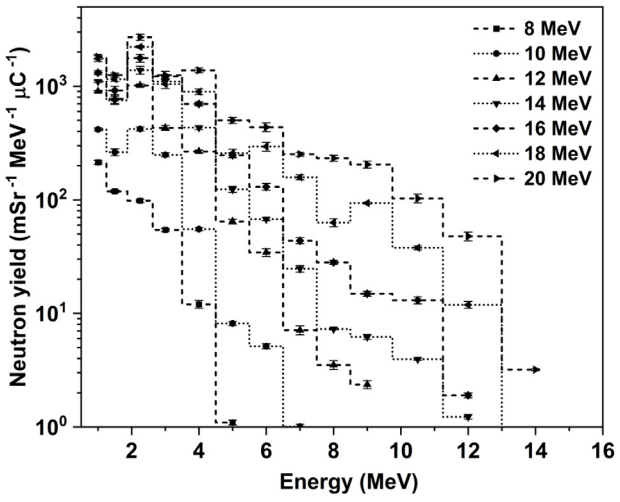

Fig. 3. Measured thick target neutron yield from ^{nat}C(p, n) system at 0° with respect to the incident beam direction (Incident proton energy ranging from 8–20 MeV with 2 MeV interval).

only 0.67 MeV and have experimentally measured neutron emission cross-sections (~300 mb at 1.3 MeV) in the proton energy range till 1.5 MeV [5,22], which are available at higher energies with TENDL [23] evaluations. But contribution from this pathway is also insignificant due to very low abundance fraction.

For ^{12}C based pathways, both (p,n) and (p,np) have very high threshold and the measured cross-sections are also too small in the energy range under study. In case of ^{12}C (p,n) reactions, the measured cross-section was reported to be only 3.45 ± 0.49 mb at 25.8 MeV [24]. The red dots in Fig. 2 indicates the cross-section for ^{12}C (p, np) reactions. The Blue marking are presented for visual guidance about the average measured cross-sections with increasing proton energy. The plot refers that cross-sections are considerable only beyond proton energies of 20 MeV. So the neutron yield contributions from the ^{12}C isotopes can be neglected in the proton energy range of 8–20 MeV and ^{13}C(p, n) reaction remains as the dominant contributor.

3.1. Study of thick target neutron spectra

The thick target neutron spectra measured at 0° and 90° angles using the neutron spectrometer are shown in Figs. 3 and 4 respectively.

Double differential neutron yields were converted to units of (mSr^{-1}) per unit μC charge of incident protons at a specified energy. The measured neutron energy maxima confirms the contribution from ^{13}C(p, n) reaction, as these end point energies are found to be nearly 3–4 MeV less compared to the incident proton energy considering the Q-value of the reaction. In case of 8 MeV protons, the neutron spectra steadily decreased at higher neutron energies. With increasing proton energies, a peaking around 1–2 MeV was observed and the high energy neutron yields progressively increased.

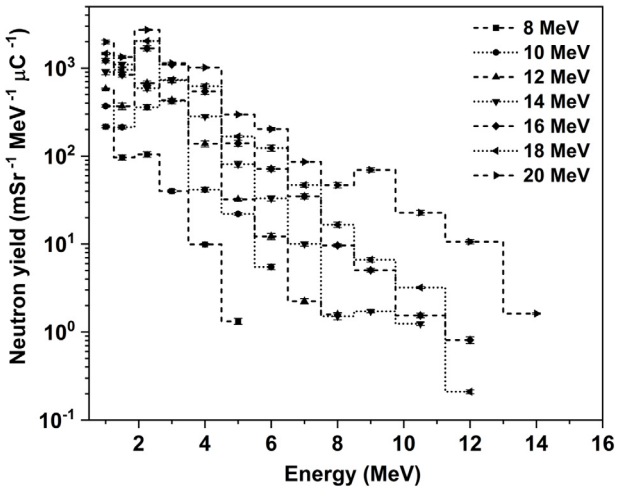

Fig. 4. Measured thick target neutron yield from ^{nat}C(p, n) system at 90° with respect to the incident beam direction (Proton energy ranging from 8–20 MeV at 2 MeV interval).

The spectra at 90° (Fig. 4) showed a similar trend with much softer neutron spectra compared to 0° measurements. At both angles, the yield reduces steadily with increasing neutron energies but at 0° measurements, the neutron fraction at intermediate neutron energies were found to be higher compared to 90° measurements. It can also be observed that, the contribution of the intermediate energies becomes prominent at higher proton energies. For quantification of the average

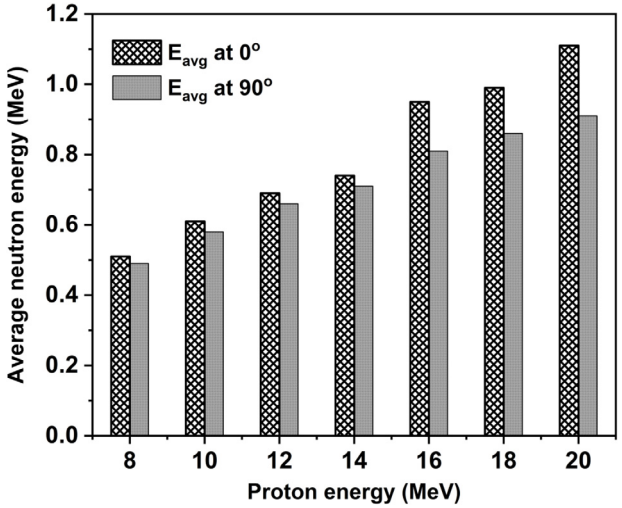

Fig. 5. Average neutron energy from the thick target ^{nat}C(p, n) system at 0° and 90° with respect to the incident beam direction.

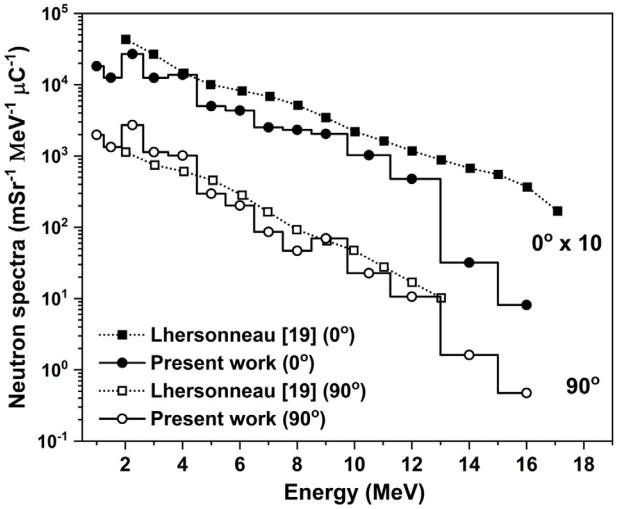

Fig. 6. Comparison of measured thick target neutron spectra from ^{nat}C(p, n) system at 20 MeV proton energy in 0° and 90° directions with the present experiment and the measurements reported by Lhersonneau et al. [19] adjusted for natural abundance of ^{13}C.

neutron energy at specific proton energy, the fluence weighted average neutron energy was estimated from the measured neutron spectra at both angles. The incident proton energy versus neutron energy plots at 8–20 MeV are shown in Fig. 5. This acts as the average emission neutron energy indicator at both angles. The average neutron energy of the neutrons at 0° indicated higher value compared to 90°. At lower proton energies up to 14 MeV, the average neutron energy variation was found to be only ~5% between both the angles. Beyond 14 MeV, the variation was found to be more than 15% in case of 16 and 18 MeV and 20% for 20 MeV protons. So, the Figs. 3–5, present the measured neutron spectra and fluence weighted average neutron energies at the incident proton energies between 8–20 MeV.

In the next part, a comparison of the neutron spectra measured in this work with the derived thick neutron spectra measurement by Lhersonneau et al. [19] is presented. In this approach, the double differential neutron spectra measured using time of flight technique with 82% enriched ^{13}C targets at 20 MeV proton bombardments on a thick stopping carbon target in units of neutrons proton^{-1} Sr^{-1}MeV^{-1} has been converted to the number of neutrons mSr^{-1}MeV^{-1} μC^{-1}. As in case of ^{nat}C(p, n) system, the major contributor is the ^{13}C(p, n) reaction, so for comparison purposes, the spectral information from Lhersonneau et al. [19] was scaled to the natural abundance of 1.07% of ^{13}C for both angles. The comparison of the scaled double differential spectra (squares) to the present measurement (circle) at 0° and 90° are shown in Fig. 6 in units of mSr^{-1} MeV^{-1} μC^{-1} of proton charge.

For a better visual representation, the 0° measurements were multiplied with a factor of 10. The present measurements showed a close corroboration with the reported neutron spectra [19] at both angles. In the forward direction (0º), the present measurements showed underestimation at higher emission neutron energies beyond 5 MeV. Above 10 MeV, the neutron yield reduced sharply by an order of magnitude compared to the spectra reported by Lhersonneau et al. [19]. In the backward direction (90º), the present measurements showed nearly two times higher yield at the 2 MeV emission neutron beam. Except this energy point, the present measurement showed a close corroboration with the earlier measurements [19].

3.2. Measurements of thick target neutron yield

The total thick target neutron yield from the ^{nat}C(p, n) system are shown in Fig. 7. The measured neutron yields at 0° direction were found to increase from 6.16 × 10^2 to 1.29 × 10^4 neutrons mSr^{-1}μC^{-1} for 8 to 20 MeV protons. Correspondingly at 90°, the variation was from 4.69 × 10^2 to 8.92 × 10^3 neutrons mSr^{-1} μC^{-1}. So effectively with the increase in proton energy from 8 to 20 MeV, the neutron yields increased nearly 21 times in the forward direction, whereas at 90° direction, the increase was nearly 13 times. The neutron yields at 0° and 90° are presented with solid squares and circles respectively with associated uncertainties in the measurements. The cumulative uncertainties were estimated to be around 5%–9% based on the statistical and measurement uncertainties together. In the measurement uncertainty, the error in target thickness, weight and beam parameters (energy resolution, beam energy spread, beam shape fluctuations etc.) were included. The representative curves joining the data points are only for visual guidance.

The measured total thick target neutron yields were compared with the similar experiments using infinitely thick carbon targets. The neutron yield measurements carried out by Bair et al. [14] and thin target neutron emission cross-section measurements reported by Dagley et al. [15] were converted for comparison with the present measurements. A theoretical estimate of the total neutron yield by Chaudhri [16] in the 4π geometry till 12 MeV protons on infinitely thick natural carbon target has also been compared. The spectra at both angles obtained from Lhersonneau et al. [19] at 20 MeV were also converted to the total yields and compared with the present measurements.

The reported data from Bair et al. [14] and Dagley et al. [15] overestimated the neutron yields compared to the present measurements in the proton energy range of 8–12 MeV, whereas the theoretical yield estimates prescribed by Chaudhri [16] were closely reproduced in the present experiment. The sole measurement available at 20 MeV by Lhersonneau et al. [19] provided a very close match with the yields at 0° direction. In case 90° measurements, though the spectrum comparison showed a close corroboration in Fig. 6, but the total yield indicates a large underestimation. This attributes to the additional low energy neutron yields at neutron energy bins below 2 MeV in the present measurements.

3.3. Thick target neutron dose measurements

The neutron ambient dose equivalent $H^*(10)$ for the ^{nat}C(p, n) system at different proton energies were measured using a neutron dose equivalent (NDE) rem meter at both 0° and 90° directions with respect to the incident beam at a distance of 135 cm from the target–projectile interaction point are shown in Fig. 8 in units of μSv per unit μC charge.

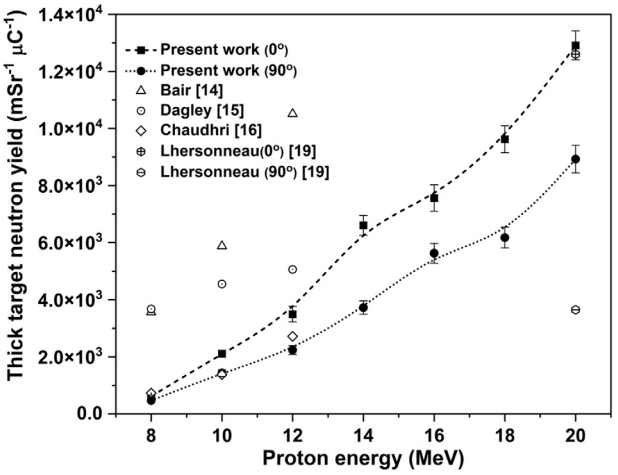

Fig. 7. Comparison of thick target neutron yields between proton (8–20 MeV) interaction with a thick ^{nat}C target and the reported theoretical and experimental measurements.

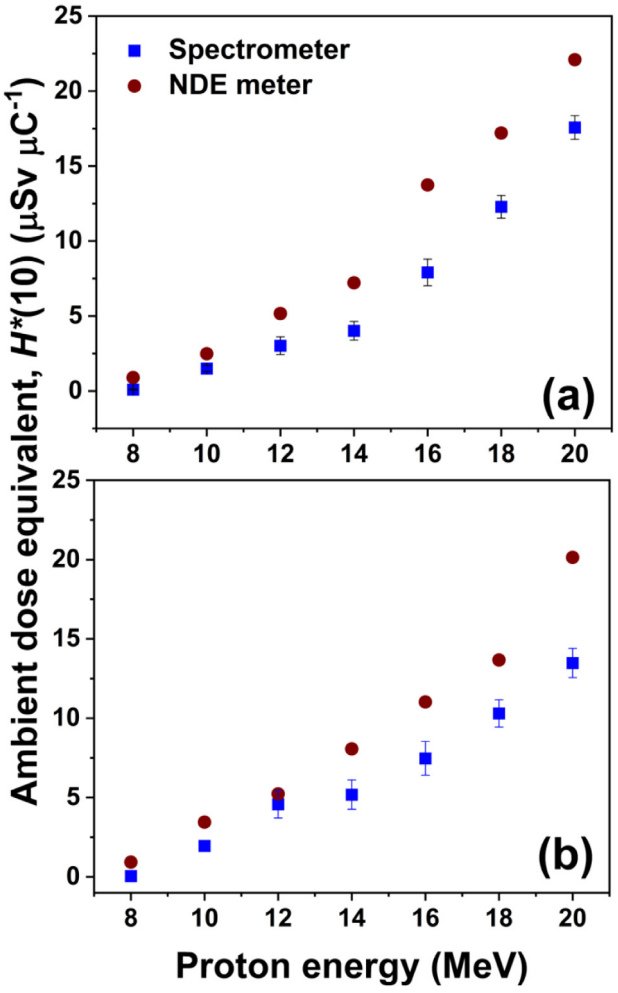

Fig. 8. Measured neutron ambient dose equivalent, $H^*(10)$ at 135 cm from the reaction point for ^{nat}C(p, n) system with proton energies between 8–20 MeV using the conventional NDE meter and neutron spectrometer at (a) 0° and (b) 90° directions.

A second dosimetric measurement has been carried out using the scintillator based neutron spectrometer at the same distance with and without the shadow bar. For both the instruments, the neutron to gamma rejection ratio is >300:1 and as a result, though the detectors have finite probability of interaction to the high energy photons, but the detected dose equivalent can be considered primarily from neutron interactions. For NDE meter measurements no shadow bar was used and the neutron dose incorporates the contribution of scattered neutrons from the structural and shielding materials available in the near vicinity of the target–projectile interaction volume. The NDE meter measurements were found to vary from 0.9 μSv μC^{-1} for 8 MeV protons to 22.09 μSv μC^{-1} for 20 MeV at 0° direction whereas in the 90° direction, the maximum measured dose was 20.14 μSv μC^{-1} for 20 MeV. In the 0° direction at lower proton energies till 12 MeV, both NDE meter and neutron spectrometric measurements have shown similar values indicating small contribution from low energy scattered neutrons from structural or nearby shielding materials. The variations were found significant at both angles for proton energies beyond 12 MeV and the NDE meter measurements were found conservative. This measured dose variations between the two approaches can be attributed to the scattering fractions. In case of spectra based estimates, the scattered fractions could be eliminated, based on the shadow bar measurements. But in case of dosimetric applications, the NDE meter measurements are preferred.

The scattering subtracted spectrometric measurements after shadow bar correction can be referred as the "true" or net neutron dose from the ^{nat}C(p, n) system at both angles. In this case, the neutron fluence spectra were folded with ICRP-74 [25] dose conversion co-efficient to estimate the dose equivalent $H^*(10)$. The spectrometric measurements at 0° were found to vary from 0.09 to 17.57 μSv μC^{-1} for proton energy variation between 8 to 20 MeV. At 90°, the measured variation was between 0.05 to 13.48 μSv μC^{-1}.

4. Conclusions

Present measurement provides the thick target neutron yields, neutron spectra and ambient dose equivalent $H^*(10)$ from the ^{nat}C(p, n) system at proton energies between 8–20 MeV with an energy interval of 2 MeV. All the parameters were measured at 0° and 90° directions with respect to the incident proton beam. The conclusions derived from the present study are summarized below:

- In case of natural carbon target, the primary contributor to the neutron yield is the ^{13}C(p, n) reaction in the proton energy range between 8–20 MeV.
- Measured total neutron yield was found nearly 40% higher in the 0° direction compared to 90° with respect to the incident proton beam.
- The neutron yields were found to vary from 6.16×10^2 to 1.29×10^4 neutrons mSr^{-1} μC^{-1} in the 0° direction and 4.69×10^2 to 8.92×10^3 neutrons mSr^{-1} μC^{-1} in the 90° directions.
- Average neutron energies were found to increase progressively with increase in the incident proton energy and beyond 14 MeV, the average energy in the 0° direction increased significantly over 90° direction indicating enhanced contribution of the high energy neutrons in the forward angle.
- Neutron dose equivalent meter was also used for neutron dose measurements at 135 cm from the ^{nat}C(p, n) system. The conservative estimates of the neutron doses were found to vary between 0.9 μSv μC^{-1} to 22.09 μSv μC^{-1} at 0° direction for 8 to 20 MeV incident protons. The maximum dose in the 90° directions was found to be 20.14 μSv μC^{-1}.
- Dose measurements after subtracting the scattering contributions using shadow bar measurements were found to vary between 0.09 to 17.57 μSv μC^{-1} at 0° and 0.05 to 13.48 μSv μC^{-1} at 90° for proton energies between 8 to 20 MeV.

These measurements will help in estimating the net neutron yields from the backing materials in case of proton induced studies on low Z target materials with natural graphite blocks as the supporting material. As,

the available measurements with the present system were restricted mostly up to 12 MeV with a natural infinitely thick carbon target and few sparse measurements are available beyond 20 MeV, so, this study will supplement the measurement void as regards to the emission neutron parameter studies for the ^{nat}C(p, n) reaction system between 12–20 MeV incident proton energies.

CRediT authorship contribution statement

Sabyasachi Paul: Conceptualization, Investigation, Formal analysis, Writing – original draft. **Meghnath Sen:** Investigation, Formal analysis. **S.S. Ghodke:** Investigation, Formal analysis. **A.A. Shanbhag:** Investigation. **S.P. Tripathy:** Conceptualization, Writing – review & editing, Visualization. **G.S. Sahoo:** Investigation. **S.C. Sharma:** Resources. **N.G. Ninawe:** Resources. **Y. Singh:** Investigation. **R.B. Rakesh:** Resources. **M.S. Kulkarni:** Writing – review & editing, Supervision, Project administration.

Declaration of competing interest

The authors declare that they have no known competing financial interests or personal relationships that could have appeared to influence the work reported in this paper.

Acknowledgments

Authors would like to acknowledge the staff members of the Pelletron-LINAC facility for their support during the experiments. SP would like to acknowledge Dr. V Sathian, Head, Radiation Standards Section and Shri P. Chaudhury, Head, Radiation Safety Systems Division, BARC for their support during the course of this work.

References

[1] M.A. Blackston, P.A. Hausladen, Fast-neutron elastic-scatter imaging for material characterization, in: Proc. IEEE Nuclear Science Symposium and Medical Imaging Conference, 2015, pp. 1–9, http://dx.doi.org/10.1109/NSSMIC.2015.7581846.

[2] J. Spencer, S. Anderson, Z. Wolf, J. Volk, D. Pellett, D., M. Boussoufi, Fast Neutron Radioactivity and Damage Studies on Materials, UCD McClellan Nuclear Radiation Center, UC Davis, 2007, https://escholarship.org/uc/item/6kr8z43b.

[3] R. Nolte, M.S. Allie, P.J. Binns, F. Brooks, A. Buffler, V. Dangendorf, J.P. Meulders, F. Roos, H. Schuhmacher, B. Wiegel, High-energy neutron reference fields for the calibration of detectors used in neutron spectrometry, Nucl. Instrum. Methods Phys. Res. A 476 (2002) 369–373, http://dx.doi.org/10.1016/S0168-9002(01)01472-3.

[4] J.H. Gibbons, R.L. Macklin, Total neutron yields from light elements under proton and alpha bombardment, Phys. Rev. 114 (1959) 571–580.

[5] C. Wong, J.D. Anderson, S.D. Bloom, J.W. Mcclure, B.D. Walker, Angular distribution of the ground-state Neutrons from the C^{13}(p, n)N^{13} and N^{15}(p, n)O^{15} reactions, Phys. Rev. 123 (1961) 598–605.

[6] Sabyasachi. Paul, G.S. Sahoo, S.P. Tripathy, S.C. Sharma, D.S. Joshi, T. Bandyopadhyay, Measurement of thick target neutron yield from the reaction (p + 181Ta) with projectiles in the range of 6-20 MeV, Nucl. Instrum. Methods Phys. Res. A 880 (2018) 75–79.

[7] Sabyasachi. Paul, G.S. Sahoo, S.P. Tripathy, S.C. Sharma, D.S. Joshi, M.S. Kulkarni, Neutron measurements from the interaction of a thick ta target with protons at different energies, Nucl. Instrum. Methods Phys. Res. A 957 (2020) 163432.

[8] Sabyasachi. Paul, S.P. Tripathy, G.S. Sahoo, S.C. Sharma, D.S. Joshi, M.S. Kulkarni, Thin target neutron yield for Li(p, n) reaction with thick ta target as stopping material, Nucl. Instrum. Methods Phys. Res. A 981 (2020) 164561.

[9] J.K. Bair, C.M. Jones, H.B. Willard, Neutrons from the proton bombardment of Li6, Li7, Be9, B11 and O15, Nucl. Phys. 53 (1964) 209–218.

[10] H. Schuhmacher, H.J. Brede, V. Dangendorf, M. Kuhfuss, J.P. Meulders, W.D. Newhauser, R. Nolte, Quasi-monoenergetic neutron beams with energies from 25 to 70MeV, Nucl. Instrum. Methods Phys. Res. A 421 (1999) 284–295, http://dx.doi.org/10.1016/S0168-9002(98)01267-4.

[11] Y. Uwamino, T.S. Soewarsono, H. Sugita, Y. Uno, T. Nakamura, T. Shibata, M. Imamura, Sei-ichi. Shibata, High-energy p-Li neutron field for activation experiment, Nucl. Instrum. Methods Phys. Res. A 389 (1997) 463–473, http://dx.doi.org/10.1016/S0168-9002(97)00345-8.

[12] M. Majerle, P. Bém, J. Novák, E. Šimečková, S.P. Simakov, U. Fischer, Validation of 59Co and 93Nb activation cross sections in a quasi-mono energetic neutron spectrum (35 MeV) including irradiation, in: Measurement and Computational Analysis, International Atomic Energy Agency, Vienna, Austria, 2016, https://www-nds.iaea.org/publications/indc/indc-czr-0002/.

[13] Héctor René Vega-Carrillo, Neutron energy spectra inside a PET cyclotron vault room, Nucl. Instrum. Methods Phys. Res. A 463 (2001) 375–386, http://dx.doi.org/10.1016/S0168-9002(01)00234-0.

[14] J.K. Bair, P.D. Miller, B.W. Wieland, Neutron yields from the 4-12 MeV proton bombardment of^{11}B,^{13}C and^{18}0 as related to the production of^{11}C,^{13}N and^{18}F, Int. J. Appl. Radiat. Isot. 32 (1981) 389–395.

[15] P. Dagley, W. Haeberli, J.X. Saladin, The C^{13}(p, n)N^{13} reaction cross section from threshold to 13 MeV, Nucl. Phys. 24 (1961) 353–371.

[16] M.A. Chaudhri, Neutron productions from carbon by charged particle bombardment at different energies, in: M.K. Craddock, G. Dutto (Eds.), Proc. XIII International Conference on Cyclotrons and their Applications, World Scientific, Singapore, ISBN: 9810211309, 1993, pp. 178–180.

[17] G. Lhersonneau, T. Malkiewicz, M. Fadil, D. Gorelov, P. Jones, P.Z. Ngcobo, J. Sorri, W.H. Trzaska, Neutron yield of thick 12C and 13C targets with 20 and 30 MeV deuterons, Eur. Phys. J. A 52 (2016) 364, http://dx.doi.org/10.1140/epja/i2016-16364-x.

[18] O. Alyakrinskiy, A. Andrighetto, M. Barbui, S. Brandenburg, M. Cinausero, B. Dalena, P. Dendooven, E. Fioretto, G. Lhersonneau, W. Lyapind, G. Prete, G. Simonetti, L. Stroe, L.B. Tecchio, W.H. Trzaska, Neutron yield from a thick 13C target irradiated by 90MeV protons, Nucl. Inst. Methods Phys. Res. A 547 (2005) 616.

[19] G. Lhersonneau, T. Malkiewicz, D. Vakhtin, V. Plokhoi, O. Alyakrinskiy, M. Cinausero, Ya. Kandiev, H. Kettunen, S. Khlebnikov, H. Penttilä, G. Prete, V. Rizzi, S. Samarin, L. Tecchio, W.H. Trzaska, G. Tyurin, Neutron yield from a 13C thick target irradiated by protons of intermediate energy, Nucl. Instrum. Methods Phys. Res. A 576 (2007) 371–379, http://dx.doi.org/10.1016/j.nima.2007.02.106.

[20] James F. Ziegler, M.D. Ziegler, J.P. Biersack, SRIM – the stopping and range of ions in matter, Nucl. Instrum. Methods Phys. Res. Section B 268 (2010) 1818–1823, http://dx.doi.org/10.1016/j.nimb.2010.02.091.

[21] V.V. Zerkin, B. Pritychenko, The experimental nuclear reaction data (EXFOR): Extended computer database and web retrieval system, Nucl. Instrum. Methods Phys. Res. A 888 (2018) 31–43, http://dx.doi.org/10.1016/j.nima.2018.01.045.

[22] T.R. Wang, R.B. Vogelaar, R.W. Kavanagh, 11B+α Reaction rates and primordial nucleosynthesis, Phys. Rev. C 43 (1991) 883.

[23] A.J. Koning, D. Rochman, J. Sublet, N. Dzysiuk, M. Fleming, S. van der Marck, TENDL: Complete nuclear data library for innovative nuclear science and technology, Nucl. Data Sheets 155 (2019) 1.

[24] S.D. Schery, D.A. Lind, H.W. Fielding, C.D. Zafiratos, The (p,n) reaction to the isobaric analogue state of high-Z elements at 25.8 MeV, Nuclear Phys. A 234 (1974) 109–129.

[25] Conversion coefficients for use in radiological protection against external radiation, international commission on radiological protection, ICRP publication 74, Ann. ICRP 26 (3–4) (1996).